Assessment of Mechanical Robustness and Resilience in Urban Water Networks Under the Impact of Climate Change Using Metamodels and Artificial Intelligence

Minh Tuan Bui[1]

[1] *Researcher/Ph.D. Candidate, University of Bordeaux, Arts et Metiers Institute of Technology, CNRS, Bordeaux INP, I2M, UMR 5295, F-33400, Talence, France, email: minh-tuan.bui@u-bordeaux.fr*

Abstract: Urban water networks play a crucial role in urban functionality. These systems are indispensable elements of urban resilience. However, these long-established systems are facing challenges due to global population growth, urbanization, and climate change. These challenges reduce the mechanical robustness and resilience of these aging systems as an inevitable consequence. This study proposes a metamodeling approach to determine the indices of robustness and resilience from a mechanical point of view by conducting a study on various 3D soil-pipe configurations under the effect of climate change. These configurations are identified on an experimental basis, especially using a central composite design to build the metamodel, whereas a sensitivity analysis will identify the most important inputs. Machine learning models are the alternative predictive modeling tool that can be used instead of computationally heavy traditional simulations. The computational efficiency offered by the modeling approach therefore allows a more rapid evaluation of a larger number of scenarios, even scenarios that are not explicitly represented in the datasets of original mechanical indicators. Thus, this approach eventually finds the critical pipes and provides the mechanical robustness and resilience of the overall water network, thereby supporting the decision-makers in managing these systems.

Keyword(s): Water Infrastructure, Sensitivity Analysis, Monte Carlo Simulation, Machine Learning, Decision-Making Support.

I. INTRODUCTION

The urban water network (UWN) is a vital lifeline sustaining any community in normal functioning and is considered integral to city resilience (Rodríguez et al., 2021). When water allocation capacity is affected, imbalances in water supply and demand result, leading to increased vulnerability to water shortages and droughts, increased costs, and environmental damage (He et al., 2021). Loss of water pressure and maintainability leads to water leakage, significantly affecting people's activities (Bata et al., 2022). Unfortunately, these aging structures are heavily influenced by global population growth, the rapid development of urban areas (Castells-Quintana and Wenban-Smith, 2020), and the unpredictable complexity of climate change (Demuzere et al., 2014). Given the importance of UWN, optimizing urban infrastructure resilience to adapt to extreme events is crucial. To improve decision support for UWN, this study introduces a novel methodology from the engineer's perspective. In this study, based on the engineer's point of view and on physical factors, urban water robustness (UWR_b) signifies the mechanical strength of UWN when subjected to climate change, while urban water resilience (UWR_e) means the mechanical performance of UWN with respect to time. Recent research (Bui et

al., 2025) shows that artificial intelligence (AI) is indeed showing some success in predicting parameters with the hydraulics and physics of UWN systems. Another research study (Yanez-Godoy and Elachachi, 2023a) found that metamodels effectively handle geotechnical parameters when applied to soil-pipe systems. This methodology analyzes UWR_b and UWR_e using metamodels based on AI and mechanical probabilistic modeling within a representative section of a network. The first section of this study presents the full methodology, which includes data collection, 3D geomechanical simulation with climate change assessment, sensitivity analysis, experiment design, predictive modeling, data generation using metamodel, and UWR_b and UWR_e assessment. The second section covers the results and discusses them. The final section is the conclusion.

II. METHODOLOGY

Figure 1 shows the overview steps for assessment of mechanical robustness and resilience in UWN in response to climate change using metamodels:

FIGURE 1. Overview of the methodology.

A. Database

A linear UWN topology with 5 pipes and 6 nodes is introduced as the database (see Figure 2a). The numbering of nodes is based on the fact that the node [0] represents the water tank so that the numbering starts from [0], which also means that the water flows along a single path from node [0] to the next linear nodes and stops at node [5]. Each edge of this network is represented by one pipe, while the nodes are the corresponding valves controlling water flow. Various mechanical parameter datasets are stored in each pipe; these data are obtained from the metamodel in the following step. The important parameters will be considered based on sensitivity analysis results. A dataset has been collected for the modelling step, including among others all the necessary key parameters (Yanez-Godoy and Elachachi, 2023a). This includes data on geometric and mechanical characteristics of the pipes, geomechanical properties, external and internal loading imposed on UWN (see Figure 2b). Each pipe has a common fixed length of 18 m.

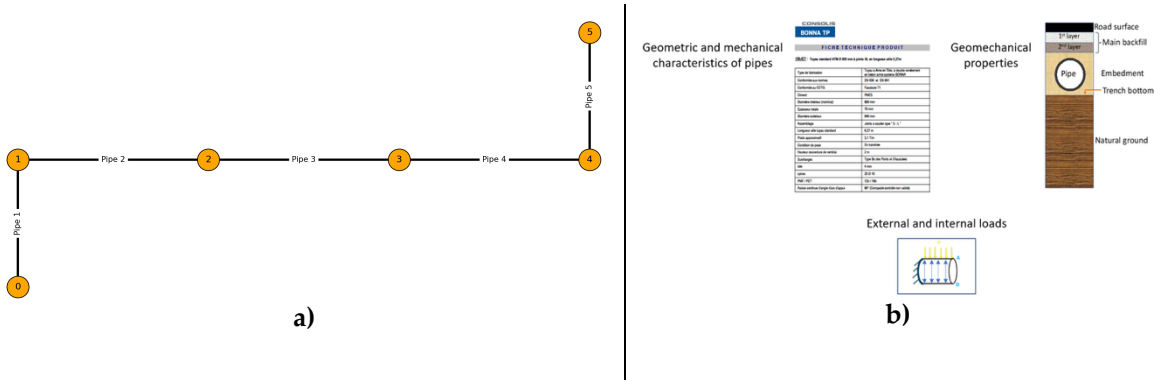

FIGURE 2. Overview of the database.

B. 3D Geomechanical Simulation & Climate Change Impact Simulation

This study used the UWN simulation approach with geomechanical modeling to model buried infrastructure. Each 3D model was developed within OpenSeesPy (Zhu et al., 2018) to implement the finite element analysis in Python. The geometry and mesh of the finite elements for the models were created using the software Gmsh (Geuzaine and Remacle, 2009). Two different materials are used here in complement: one is linear for the pipes, and the other is non-linear for modeling the soil layers by the Drucker-Prager model. The non-linear model allows the modification of the elastic function so that singularities related to the internal friction angle may be avoided. Each model consists of 4 layers: Main Backfill & Embedment Layer, Pipeline, Bedding, and Natural Ground.

Regarding climate change, Dong and Lu, 2017 showed that Young's modulus increased when the soil was dry and decreased when the soil was moist, related to humidity due to climate change. Lu et al., 2019 examined the impact of freeze-thaw cycles on expansive soils, showing that the Young's modulus decreased significantly at the first cycle and gradually stabilized as the number of cycles increased. Yang et al., 2024 investigated the impact of freeze-thaw cycles on the mechanical properties of riverbank soil in cold regions, showing that the Young's modulus of the soil decreased significantly as the number of freeze-thaw cycles increased, with a decrease of 40.84% to 68.70% after 10 cycles at freezing temperatures from -5°C to -20°C. From the conclusions from those studies, to simulate climate change, Young's modulus (E) was randomly varied in the Natural Ground layers after the sensitivity analysis step. Figure 3 shows a representative 3D soil-pipe model with 4 layers and a load in the middle of the pipe:

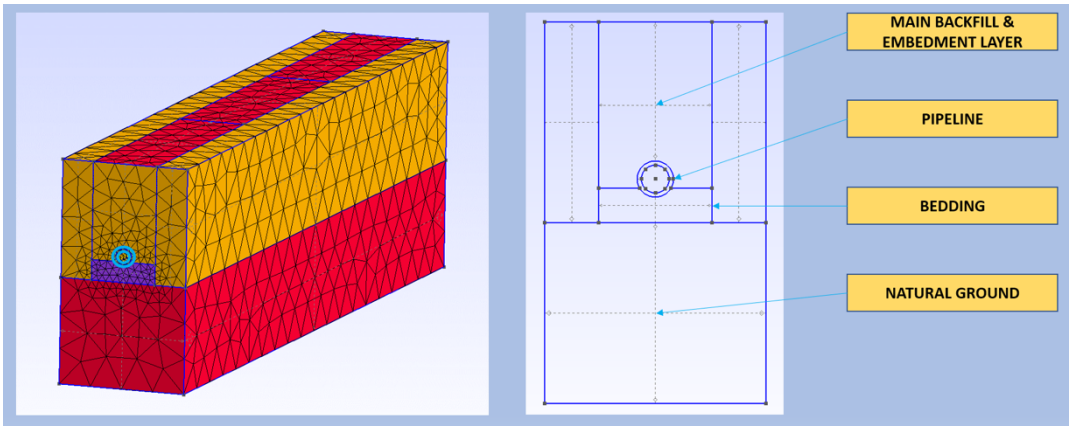

FIGURE 3. The 3D soil-pipe model has four layers with the load in the middle of the pipe. The fixed length for the pipe of all models is 18 m. The characteristics of each model of the metamodel are given in the following step.

C. Sensitivity Analysis

Modeling 3D geomechanical systems involves numerous input factors, but some have little impact on model outputs. To determine which factors are most important, Global Sensitivity Analysis (GSA) is employed based on the Morris method (Morris, 1991), which is one of the simplest classes of screening designs (called one-at-a-time OAT experiments). The Morris method

that defines the elementary effect d_i of the x_i factor in the *k*-dimensional factor vector X can be expressed as follows (Saltelli et al., 2008):

$$d_i(x_i) = \frac{Y(x_1,\dots,x_{i-1},x_i+\Delta,x_{i+1},\dots,x_k)-Y(X)}{\Delta} \quad \textbf{(Eq. 1)}$$

Where x_i is any value in the region of experimentation Ω (which is a *k*-dimensional *p*-level grid) selected such that the perturbed point $x_i + \Delta$ is still in Ω; Δ is a predetermined multiple of $\frac{1}{p-1}$; p is the number of values in the set $\left\{0,\frac{1}{p-1},\frac{2}{p-1},\dots,1\right\}$; Y is the output; k is the number of input parameters. A finite distribution F_i of elementary effects for the x_i input factor is then obtained by sampling X from Ω. The total computational effort required for a random sample of r values from each distribution F_i is $n = r(k+1)$ runs. The characterization of F_i through its mean, μ^*, and standard deviation, σ, gives useful information about the influence of the x_i factor on the output. A high μ^* indicates a factor with an important overall influence on the output. A high σ indicates that the factor in question may be interacting with other variables or that its effect is non-linear.

D. Metamodel based on Artificial Intelligence

Design of Experiments (DOE) (Fisher, 1936) concerns the design of any task that attempts to describe and explain the variance of information under hypothetical conditions. Basically, the experiment will be set up with the objective to predict outputs by means of changing the preconditions, otherwise called input factors. DOE constitutes a structured approach that allows users to study the relationship between multiple input variables and a few key output variables, with the advantage of requiring a minimal amount of experimentation or input data. DOE herein is the basis employed to run the UWN metamodels.

AI, and more specifically Machine Learning (ML), has a significant impact on transforming ecosystems because this technique is highly relevant for future technologies (Howard, 2019). According to the recent studies (Bui et al., 2025), such technologies can be applied robustly to UWN while considering both physical and hydraulic parameters for application in many cases with many different models and data sets. Within this study, ML is used as a predictive modeling tool to implement the metamodel. Numerical models for assessing UWN's mechanical strength require considering multiple outputs. This study demonstrates this approach by predicting the maximum displacement (δ_{max}) and Von Mises stress (σ_{vm}) of pipes under service loads. The DOE matrix developed earlier provides the input data for the 3D model calculations.

The Central Composite Design (CCD) method was used to conduct the DOE and can be represented as follows (Yanez-Godoy and Elachachi, 2023b):

$$N_T = n_f + n_a + n_0 \quad \textbf{(Eq. 2)}$$

Where N_T is the total number of points for an orthogonal design, the factorial portion is $n_f = 2^{\kappa-1}$, the number of axial points is $n_a = 2\kappa$, and n_0 is the number of center points. The total number of factors κ is determined in the previous section.

E. Assessment of Mechanical Robustness and Resilience of Urban Water Network

Regarding the concept of "Robustness" when referring to structures, according to EN 1991-1-7 Eurocode 1 (EN, 1991), it can be defined as: "*The ability of a structure to withstand events like fire, explosions, impact, or the consequences of human error without being damaged to an extent disproportionate to the original cause.*" On the other side, according to UNDRR ("Resilience | UNDRR," 2017), the concept of "Resilience" can be defined as: "*The ability of a system, community, or society exposed to hazards to resist, absorb, accommodate, adapt to, transform, and recover from the effects of a hazard in a timely and efficient manner, including through the preservation and restoration of its essential structures and functions through risk management.*" Indices based on these two concepts are also calculated based on different scenarios when it comes to structures (Stochino et al., 2019). In this study, "Robustness" refers to the structural robustness or mechanical resistance index of buried water infrastructure, determined based on the system's resistance (based on predictions) in the face of extreme fluctuations in simulation data in previous steps. And "Resilience" refers to the operational performance over time in a mechanical context of the entire network.

The following formula represents how urban water mechanical robustness is determined:

$$UWR_b = \frac{1}{(1+S)} \quad \textbf{(Eq. 3)}$$

Where: S represents the relative change in the combined mechanical indicator (CMI) of an edge under a 1.5 times load increase, which is a weighted combination of (δ_{max} and σ_{vm}), while UWR_b denotes the robustness index of the pipe in the network. UWR_b values are normalized to the range [0, 1] using the Min-Max Normalization formula. The CMI is calculated using weights of 0.4 for displacement and 0.6 for stress, reflecting the emphasis on stress as per EUROCODE Ultimate Limit State (ULS) considerations. Detailed descriptions are provided in Table 1:

TABLE 1. The terms of S and UWR_b.

Term	Description	Term	*Description*
S	Represents the relative change in the CMI of a pipe when the load is increased from the initial load (P) to 1.5 times (1.5P), simulating a design load condition as per EUROCODE ULS. It is calculated as: $S = \frac{CMI_{1.5P} - CMI}{CMI}$ S indicates greater sensitivity to load changes, leading to lower robustness.	***$UWR_b \geq 0.5$ Represents a High Robustness***	Indicates that the pipe has relatively low sensitivity to load-induced changes in the CMI ($S \leq 0.5$). Pipes with $UWR_b \geq 0.5$ exhibit higher stability and are less affected by extreme mechanical fluctuations, such as increased δ_{max} and σ_{vm} under higher loads.
		$UWR_b < 0.5$ Represents a Low Robustness	Indicates that the pipe has higher sensitivity to load-induced changes in the CMI ($S > 0.5$). Pipes with $UWR_b < 0.5$ are more susceptible to mechanical fluctuations, marking them as critical segments that may require prioritized maintenance.

The following formula represents how urban water mechanical resilience is determined:

$$UWR_e = \frac{\int_{t_0}^{t_f} P(t)dt - P_{min} \times (t_f - t_0)}{P_0 \times (t_f - t_0) - P_{min} \times (t_f - t_0)} \times 100 \quad \textbf{(Eq. 4)}$$

In which: UWR_e: The urban water resilience, expressed as a percentage (%).

$\int_{t_0}^{t_f} P(t)dt$: The actual area under the performance curve from initial time t_0 to final time t_f, computed using numerical integration (trapezoid method). It represents the system's performance over time, including degradation and recovery phases.

$P_{min} \times (t_f - t_0)$: The minimum possible area, assuming the system operates at its lowest performance P_{min} throughout the time period.

$P_0 \times (t_f - t_0)$: The maximum possible area, assuming the system maintains its initial performance P_0 throughout the time period.

P(t): The mechanical performance function at time t, is defined as follows:

- $P(t) = P_0$ for $t < t_{incident}$
- $P(t) = P_{min}$ for $t_{incident} \leq t < t_{recovery}$
- $P(t) = P_{min} + [(P_0 - P_{min}) / (1 + e^{(-k(t - t_{recovery}))})]$ for $t \geq t_{recovery}$

Where: $t_{incident} = 1$: Time of incident.

$t_{recovery} = 1.5$: Time to start recovery.

$k = 0.5$: The recovery rate.

III. RESULTS AND DISCUSSION

In the beginning, a Python code was programmed to automatically generate a set of geometric features and for meshing with respect to those geometric features. Then a series of 3D geotechnical simulations, without the necessity of random values, was performed to generate the input datasets. When finished performing simulations, a GSA code was run that would select the most important parameters that influence the expected outputs (δ_{max} and σ_{vm}). The analysis results show that six factors are most influential with regard to the outputs (see Figure 4), from which the CCD matrix can be constructed. Each level was defined by the distance between each other as $a = \sqrt[4]{n_f}$, where n_f is the factorial portion, calculated from the center point of the method. This matrix is used again as input data with random values to simulate climate change and to build the metamodel.

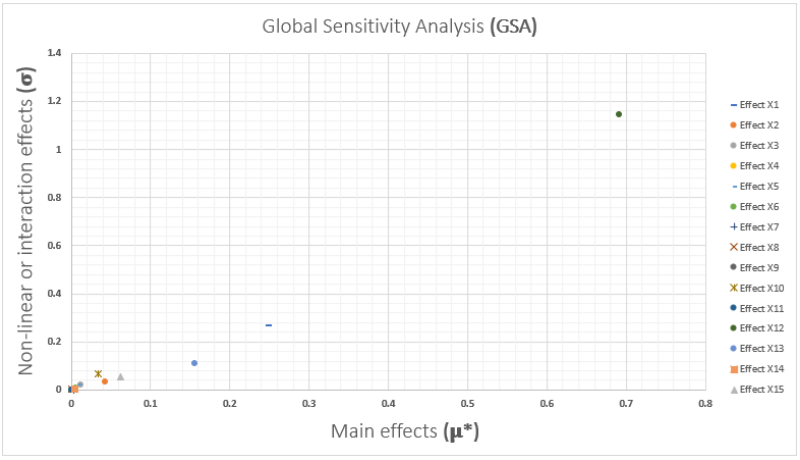

X1	Pipe geometry
X2	Pipe buried depth
X3	E of the pipe
X4	ν of the pipe
X5	Φ/ϱ of the soil layer I
X6	E of the soil layer I
X7	ν of the soil I
X8	Φ/ϱ of the soil II
X9	E of the soil layer II
X10	ν of the layer II
X11	Φ/ϱ of the soil layer III
X12	E of the soil layer III
X13	ν of the soil layer III
X14	Water pressure
X15	External force

FIGURE 4. Results of sensitivity analysis; 15 key parameters were considered, including geometrical characteristics of the pipe, buried depth of the pipe, mechanical parameters (E, ν, Φ/ϱ) of the 4 layers as in Section II, water pressure, and external forces.

Table 2 shows the performance results of the simulations obtained using the metamodel with those from the 3D geomechanical model for δ_{max} and σ_{vm}. The metamodel significantly reduced the computational time per finite element analysis, from an average of 167.25 seconds to just 0.24 seconds. Furthermore, the metamodel enabled the consideration of a broader range of possibilities than traditional methods. The model with the best performance index was used for predictive modeling of the metamodel. The model was validated using the cross-validation technique by dividing the input datasets into 5 folds; the coefficient of determination (R^2) scores from test sets served as a criterion for measuring performance of these models. The best performance of the model in this case was given by the Gradient Boosting model, which had R^2 values of 0.997 and 0.916 reported for δ_{max} and σ_{vm}, respectively. These metrics ensure a robust generalization-based predictive accuracy and model stability across various data splits. A Monte Carlo simulation was then run to generate 10,000 datasets via a beta distribution of random Young's modulus (X12). The beta distribution was chosen for its flexibility to model bounded data with various shapes, which meets the physical demands of the water network features.

TABLE 2. The performance results obtained from machine learning models.

	R^2 Score (δ_{max})	R^2 Score (σ_{vm})
Neural Network	0.765	0.754
Decision Tree	0.993	0.900
Random Forest	0.994	0.911
Gradient Boosting	0.997	0.916
Support Vector Regressor	0.976	0.863
K-Nearest Neighbors	0.983	0.873

Figure 5a with the UWN and calculated normalized UWR_b indices for every pipe portrays the varying degrees of robustness in the network. Pipe 1 shows the lowest values of robustness, with $UWR_b \approx 0.0$, indicating its being a highly critical segment vulnerable to mechanical fluctuations due to its top sensitivity to load-induced changes in the CMI. On the other hand, Pipe 3 with $UWR_b \approx 1.0$ holds the highest value of robustness, indicating its strong stability and capability to withstand δ_{max} and σ_{vm} under a 1.5 times increase in loading, possibly because of its location amid nodes [2] and [3]. Meanwhile, Pipe 2 ($UWR_b \approx 0.5$), Pipe 4 ($UWR_b \approx 0.75$), and Pipe 5 ($UWR_b \approx 0.6$) show moderately different extents of resisting operational stresses. Figure 5b shows the resilience performance over time (UWR_e), yielding a total resilience of 81.40% (normalized area under the curve). At the incident time (t = 1), the performance drops sharply down to 20% and gradually begins to recover post t = 1.5, within the repair threshold of 95%, albeit never completely approaching the initial performance of 100%. These outputs therefore emphasize that the model proposed in this paper can be used in identifying vulnerable segments of a network on a targeted basis for maintenance in order to enable UWN contractors to manage these networks under extreme conditions. However, the proposed model's estimates came from simulated data generated via Monte Carlo methods, and the possibility of biases entering should be greatly reduced if the actual distributions deviate from those assumed in the simulations, which can limit the generalizability of UWR_b indices and UWR_e estimations.

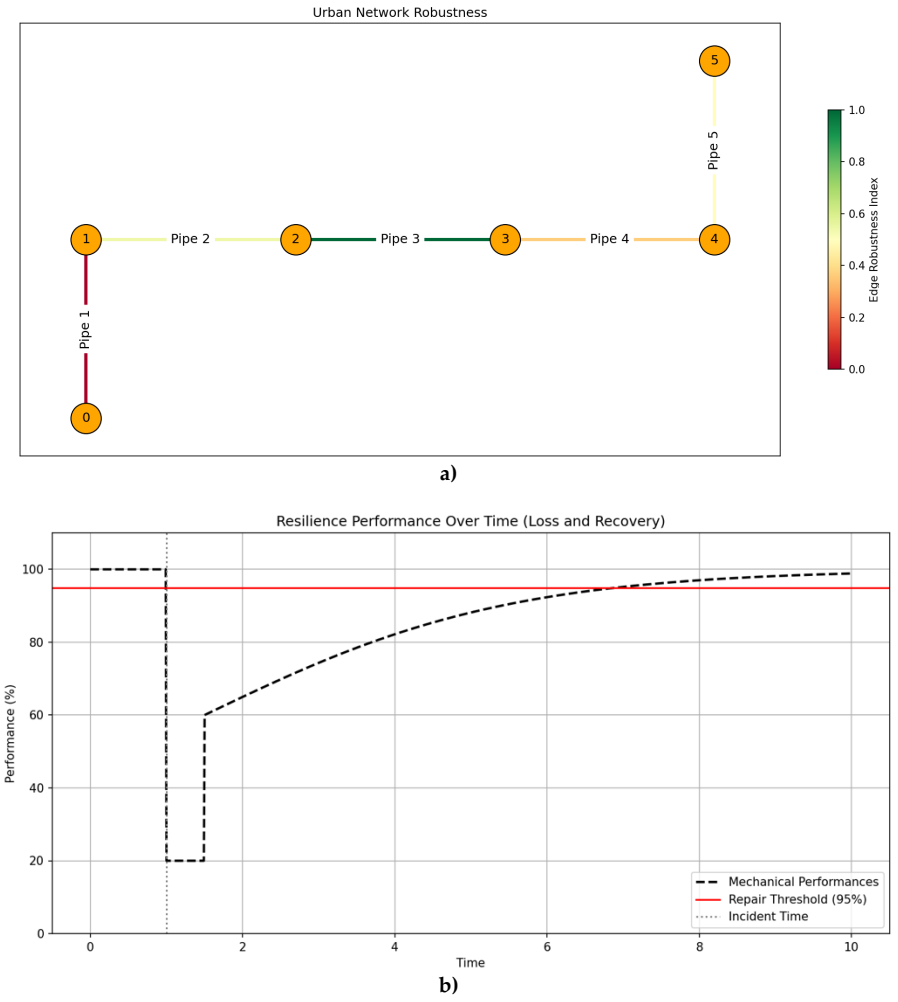

FIGURE 5. Assessment of mechanical urban water robustness (UWR_b) and urban water resilience (UWR_e) of a linear urban water network.

IV. CONCLUSION

The approach introduced in this research comprises a systematic methodology for measuring the mechanical robustness and resilience of urban water networks in response to the impacts of climate change through leveraging an artificial intelligence-based metamodel to address modern infrastructure challenges. The proposed methodology considerably reduces the complexity and costs of traditional modeling for scenario analysis beyond conventional possibilities; it combines advanced techniques such as 3D geomechanical models, design of experiments, sensitivity analysis, predictive modeling using machine learning, and Monte Carlo simulation for data generation. This framework enables not only the identification of significant pipes but also a quantitative assessment of mechanical robustness and resilience within the urban water network. Insights like these lead to a powerful, efficient tool for enabling decision-makers to act proactively against those risks posed by climate change, such as increased load stresses and unanticipated environmental events. Besides, they prioritize activities against maintenance in those sectors that are more vulnerable. It is an entirely data-centric framework, as upon its development it can be

channeled toward sustenance and resilience of water infrastructure, ensuring long-term viability and safety of urban water systems against evolving climate scenarios. Flexibility of the metamodel then also points to its possible future application in other infrastructural sectors, thus providing a basis for wider development in urban resilience and sustainability. Further research could be aimed at validating the design methodology with real datasets of urban water networks and extending it to other types of critical infrastructure, such as maintenance of gas or transportation networks.

REFERENCES

Bata, M.H., Carriveau, R., Ting, D.S.-K., 2022. Urban water supply systems' resilience under earthquake scenario. Sci. Rep. 12, 20555. https://doi.org/10.1038/s41598-022-23126-8

Bhamra, R., Dani, S., Burnard, K., 2011. Resilience: the concept, a literature review and future directions. Int. J. Prod. Res. 49, 5375–5393. https://doi.org/10.1080/00207543.2011.563826

Bui, M.T., Yanez-Godoy, H., Elachachi, S.M., 2025. Assessment of the Implications and Challenges of Using Artificial Intelligence for Urban Water Networks in the Context of Climate Change When Building Future Resilient and Smart Infrastructures. J. Pipeline Syst. Eng. Pract. 16, 03124004. https://doi.org/10.1061/JPSEA2.PSENG-1651

Castells-Quintana, D., Wenban-Smith, H., 2020. Population Dynamics, Urbanisation without Growth, and the Rise of Megacities. J. Dev. Stud. 56, 1663–1682. https://doi.org/10.1080/00220388.2019.1702160

Clédel, T., Boulahia Cuppens, N., Cuppens, F., Dagnas, R., 2020. Resilience properties and metrics: how far have we gone? J. Surveill. Secur. Saf. 1, 119–139. https://doi.org/10.20517/jsss.2020.08

Dong, Y., Lu, N., 2017. Measurement of suction-stress characteristic curve under drying and wetting conditions. Geotech. Test. J. 40, 107–121. https://doi.org/10.1520/GTJ20160058

Demuzere, M., Orru, K., Heidrich, O., Olazabal, E., Geneletti, D., Orru, H., Bhave, A.G., Mittal, N., Feliú, E., Faehnle, M., 2014. Mitigating and adapting to climate change: Multi-functional and multi-scale assessment of green urban infrastructure. J. Environ. Manage. 146, 107–115. https://doi.org/10.1016/j.jenvman.2014.07.025

EN, B., 1991. 1-7: 2006, Eurocode 1: actions on structures-Part 1-7: general actions-accidental actions . British Standards Institution, London.

Fisher, R.A., 1936. Design of experiments. Br. Med. J. 1, 554. https://doi.org/10.1136/bmj.1.3923.554-a

Geuzaine, C., Remacle, J., 2009. Gmsh: A 3-D finite element mesh generator with built-in pre- and post-processing facilities. Int. J. Numer. Methods Eng. 79, 1309–1331. https://doi.org/10.1002/nme.2579

He, C., Liu, Z., Wu, J., Pan, X., Fang, Z., Li, J., Bryan, B.A., 2021. Future global urban water scarcity and potential solutions. Nat. Commun. 12, 4667. https://doi.org/10.1038/s41467-021-25026-3

Howard, J., 2019. Artificial intelligence: Implications for the future of work. Am. J. Ind. Med. 62, 917–926. https://doi.org/10.1002/ajim.23037

Lu, Y., Liu, S., Alonso, E., Wang, L., Xu, L., Li, Z., 2019. Volume changes and mechanical degradation of a compacted expansive soil under freeze-thaw cycles. Cold Reg. Sci. Technol. 157, 206–214. https://doi.org/10.1016/j.coldregions.2018.10.008
Morris, M.D., 1991. Factorial Sampling Plans for Preliminary Computational Experiments. Technometrics 33, 161–174. https://doi.org/10.1080/00401706.1991.10484804
Ribeiro, P.J.G., Gonçalves, L.A.P.J., 2019. Urban resilience: A conceptual framework. Sustain. Cities Soc. 50, 101625. https://doi.org/10.1016/j.scs.2019.101625
Rodríguez, D.J., Paltán, H.A., García, L.E., Ray, P., St. George Freeman, S., 2021. Water-related infrastructure investments in a changing environment: a perspective from the World Bank. Water Policy 23, 31–53. https://doi.org/10.2166/wp.2021.265
Saltelli, A., Ratto, M., Andres, T., Campolongo, F., Cariboni, J., Gatelli, D., Saisana, M., Tarantola, S., 2008. Global sensitivity analysis: the primer. John Wiley & Sons. https://doi.org/10.1002/9780470725184
Stochino, F., Bedon, C., Sagaseta, J., Honfi, D., 2019. Robustness and Resilience of Structures under Extreme Loads. Adv. Civ. Eng. 2019, 4291703. https://doi.org/10.1155/2019/4291703
United Nations Office for Disaster Risk Reduction (UNDRR). 2017. The Sendai Framework Terminology on Disaster Risk Reduction. "Resilience". https://www.undrr.org/terminology/resilience.
Yanez-Godoy, H., & Elachachi, S. M. 2023a. Life-cycle assessment of buried water-transmission concrete mains. In Life-Cycle of Structures and Infrastructure Systems (pp. 3586-3593). CRC Press. https://doi.org/10.1201/9781003323020-439
Yanez-Godoy, H., Elachichi, S.M., 2023b. Decision-making tool for structural integrity assessment of buried water-transmission mains using a geomechanical approach, in: 14th International Conference on Applications of Statistics and Probability in Civil Engineering, ICASP14.
Yang, Z., Mou, X., Ji, H., Liang, Z., Zhang, J., 2024. Effects of freeze–thaw on bank soil mechanical properties and bank stability. Sci. Rep. 14, 9808. https://doi.org/10.1038/s41598-024-60698-z
Zhu, M., McKenna, F., Scott, M.H., 2018. OpenSeesPy: Python library for the OpenSees finite element framework. SoftwareX 7, 6–11. https://doi.org/10.1016/j.softx.2017.10.009